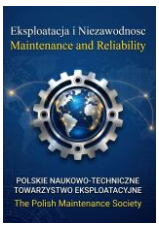

Eksploatacja i Niezawodnosc - Maintenance and Reliability

Volume 29 (2027), Issue 1

https://ein.org.pl

The Polish Maintenance Society

The influence of water and rapeseed oil on the durability of the hydraulic satellite motor

Paweł Śliwiński[1,*]

[1] Faculty of Mechanical Engineering and Ship Technology, Gdansk University of Technology, Poland
* Corresponding Author: pawel.sliwinski@pg.edu.pl

Received: 23 April 2026
Revised: 11 June 2026
Accepted: 25 June 2026
Online: 8 July 2026

Abstract

This paper describes the results of tests on the satellite motor supplied with water and edible rapeseed oil. The viscosity and density characteristics of these liquids are presented. First, the motor parameters were examined, including torque and power consumption as functions of speed for given constant pressure drops in the motor. Next, durability tests were conducted at a constant pressure drop of 20 MPa and a constant rotational speed of 1500 rpm. The motor absorbency and the torque were recorded as functions of the motor operating time. The influence of water and rapeseed oil on volumetric, mechanical, and pressure losses is presented. The relative mass loss characteristics of the working mechanism components as functions of the motor operating time, when supplied with both water and rapeseed oil, are also presented. The most rapidly wearing component of the satellite mechanism was identified.

Keywords: *non-circular mechanism, satellite mechanism, satellite motor, water, rapeseed oil*

Article citation:
Śliwiński P, The influence of water and rapeseed oil on the durability of the hydraulic satellite motor, Eksploatacja i Niezawodnosc – Maintenance and Reliability 2027: 29(1) http://doi.org/10.17531/ein/225079

Highlights

- Water and edible rapeseed oil can be used as working liquids in hydraulic systems.
- Water and rapeseed oil have different effects on motor performance.
- Water as a working liquid reduces the durability of the motor's working mechanism.
- Difference in liquid temperature in the motor provides information about its efficiency.

1. Introduction

A hydraulic motor (rotary or linear) and a positive displacement pump are the basic components of hydrostatic systems. Fixed displacement pumps driven by electric motors with frequency converters are increasingly used in hydraulic systems. By changing the rotational speed of the fixed displacement pump shaft, the pump flow rate is altered [1]. This enables variable speed operation of the hydraulic motor. This approach avoids the use of energy-inefficient throttling systems. For example, publication [2] described a system with a constant displacement pump and variable speed (the so-called EHD system). It was demonstrated that the proposed EHD system for elevator drives is more energy efficient than typical multi-valve drives [2].

The purpose of a hydraulic motor, as an actuator in a hydrostatic drive system, is to drive a specific device or machine [3]. The load on a rotary hydraulic motor is the torque M applied to its shaft, i.e., the torque required to drive the device. The effect of this load is a pressure drop Δp in the motor, i.e., the pressure difference measured at the motor's hydraulic connections [4–6].

The energy carrier in hydraulic systems is a liquid. In typical hydraulic systems, mineral oil is most commonly used as the working liquid. However, depending on the specifics and intended use of the system, other types of fluids are also used, such as synthetic fluids (HFD), synthetic fluid-in-water emulsions (HFC), oil-in-water emulsions (HFA), and water-in-oil emulsions (HFB) [7].

Water is increasingly being used as a working liquid in hydraulic systems. This requires the development of new

designs, especially positive displacement machines, that is hydraulic pumps and motors capable of operating with water. Currently, the development of piston-type machines dominates [8–11]. In addition to water and the above-mentioned liquids, attempts are being made to use hydraulic oils developed from vegetable oils [12]. Most research is focuses on rapeseed oil, which is widely available and affordable. It is refined to adapt its properties to the requirements of hydraulic systems [13–15]. Vegetable oil with a VG46 viscosity grade, typical of mineral oils, is already available on the market. This oil contains lubricating additives and is enriched with thermo-oxidising, anti-foaming and depressurising agents [15]. Attempts are also being made to use edible rapeseed oil directly in hydraulic systems. The first experimental studies using edible rapeseed oil were conducted in 2014. The object of the test was a prototype satellite motor. This motor was demonstrated to operate correctly when supplied with edible rapeseed oil [16]. However, this publication does not contain detailed information on the performance of the motor when supplied with this oil. Initial durability tests were also conducted on a satellite motor supplied with edible rapeseed oil [17]. The results of the research on this motor will be presented in the following sections of this article. More information on the influence of working pressure Δp on the load M (torque) and the absorbency Q as a function of the motor operating time τ will be presented.

Water and edible rapeseed oil are ecological liquids. Water, after all, is a common liquid on Earth. It is generally known that both rapeseed oil and water have poorer lubricating properties than mineral oil. However, water has the worst lubricating properties [15,18].

It should be noted that the satellite motor belongs to the group of satellite positive displacement machines. This group, in addition to motors, also includes satellite pumps [19–21]. The working mechanism of these machines is characterised by two elements. The outer element has non-circular internal teeth, while the inner element has non-circular external teeth (see Fig. 2 in Section 2). Satellite machine designs have been developed relatively recently. The structures of these machines' working mechanisms and their design methods have already been discussed in numerous publications, for example [22–29].

Research on satellite positive displacement machines focuses on their ability to operate with various working liquids, such as mineral oil, vegetable oil, emulsions, and even pure water. The influence of water and mineral oil on losses in satellite pumps is presented in detail in publications such as [30–31]. The influence of these liquids on losses in motors is described in works [32–34].

It should be emphasised that the effect of liquid type on the durability of hydraulic positive displacement machines has been poorly researched so far, and the literature on this topic is very limited. For example, publication [35] states that a decrease in motor speed of up to 65% and torque of up to 42% is caused by wear of the rotor surfaces in hydraulic planetary motors. Furthermore, publication [36] presents how the operating characteristics of a planetary motor change during its operation.

The durability of the satellite motor supplied with water has not yet been reported in the literature. Therefore, it was justified to conduct such durability tests. Furthermore, it is worthwhile to compare the durability test results for the motor supplied with water with those for the motor supplied with edible rapeseed oil (refined rapeseed oil). Although the durability test results for the motor supplied with edible rapeseed oil are described in detail in [17], they will also be presented in this article for ease of comparison.

The results of the satellite motor durability tests will allow assessment of the impact of water on energy losses in the motor as a function of its operating time τ under specified nominal parameters, i.e., constant pressure drop Δp in the motor and constant rotational speed n of the motor shaft. Furthermore, information will be provided on the operating time of the motor supplied with water until it is damaged or destroyed. This will enable comparison of the operating parameters of the motor supplied with water and rapeseed oil.

The influence of the geometrical and operational parameters of the satellite motor on tooth wear in the working mechanism was precisely described in publicly available work [37] and will not be discussed in this article. However, the results of material tests and the failure mechanism of the teeth of the satellite working mechanism were described in [38].

2. Satellite motor (tested motor)

The hydraulic satellite motor was the subject of the tests. The general view and structure of this motor are shown in Fig. 1 and Fig. 2.

Inside the tested motor is a type 4x6 satellite mechanism (Fig. 2). The mechanism was manufactured using the WEDM method from NIMAX tool steel. After the cutting process, the mechanism was nitrided. All parameters of this mechanism are provided in the article [37].

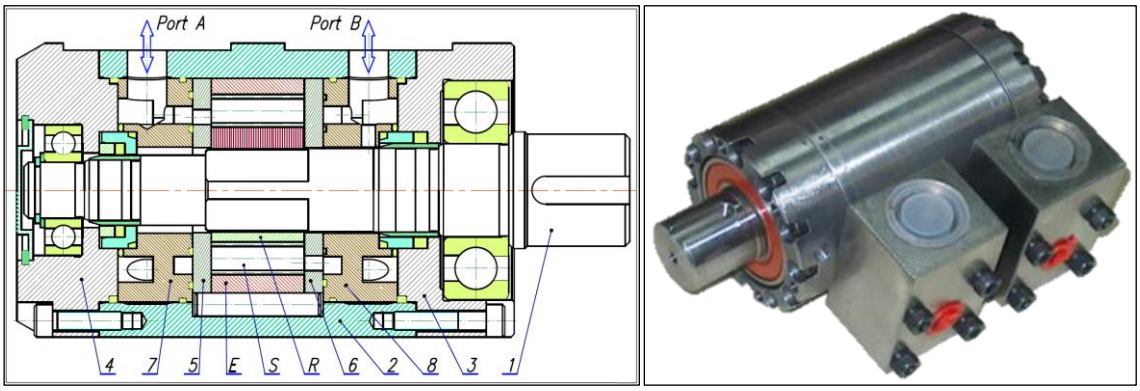

Figure 1. Tested satellite motor [17,37]: E – external gear (curvature), S – satellite, R – rotor, 1 – shaft, 2,3 and 4 – housing, 5 and 6 – commutation plates, 7 and 8 – inflow/outflow manifolds.

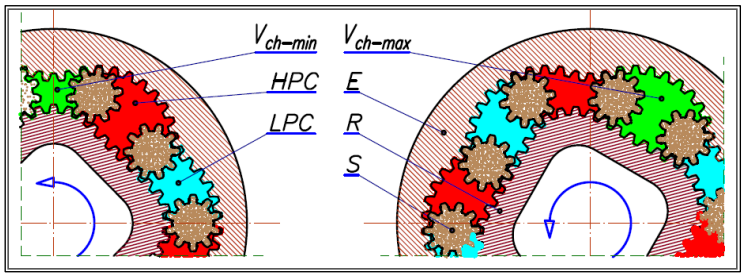

Figure 2. Satellite mechanism type 4x6 [17,39]: E – curvature, R – rotor, S – satellite, HPC and LPC – high pressure and low pressure chamber, Vch-min and Vch-max – working chambers with minimum and maximum volume.

3. Losses in the satellite motor

The following types of losses occur in hydraulic displacement machines:

a) volumetric losses;
b) mechanical losses;
c) pressure losses.

In general, the volumetric losses Q_L in positive displacement machines result from leaks and pressure differences inside the machine. Due to the volumetric losses Q_L, the actual absorbency Q of the motor is greater than the absorbency Q_r, which results directly from the actual working volume q_r and the rotational speed n of the motor shaft, i.e.:

$$Q = Q_r + Q_L \tag{1}$$

$$Q_r = q_r \cdot n \tag{2}$$

The actual working volume q_r (in [cm^3/rev]) is defined as [39,41,42]:

$$q_r = q_t + A \cdot \Delta p_i \cong q_t + A \cdot \Delta p \tag{3}$$

where:

- q_t – the theoretical working volume in [cm^3/rev];
- Δp_i – the pressure drop in the working chambers of the motor;
- Δp – the pressure drop in the motor ports (hydraulic connections);
- A – constant.

Publications [33,43] have demonstrated that, in satellite motors, volumetric losses occur in the flat gaps of the working mechanism, in the gaps of the commutation unit and in the spaces between the teeth of the cooperating elements of the satellite mechanism. The influence of the liquid parameters (kinematic viscosity ν and density ρ) on the volumetric losses is also presented in these publications.

The second type of losses in the positive displacement machine is the mechanical losses M_L. These result from the friction between the interacting elements of the motor and viscous friction in the machine gaps [34]. As a result of mechanical losses, the actual pressure drop Δp_i in the working chambers of the motor is greater than the theoretical Δp_{it}, i.e.:

$$\Delta p_i = \Delta p_{it} + 2 \cdot \pi \cdot \frac{M_L}{q_r} \quad (4)$$

$$\Delta p_{it} = 2 \cdot \pi \cdot \frac{M}{q_r} \quad (5)$$

where M is the torque on the motor shaft (the load of the motor).

The pressure drop Δp_i in the working chambers, depending on the type of displacement machine, is either impossible to measure or very difficult to measure accurately due to significant errors. It should be noted that the pressure in the working chamber is not constant, but varies from minimum to maximum with a frequency determined by the rotational speed of the machine shaft. Therefore, very often, only the pressure values measured at the connections of the tested machine are available. In such a system, it is impossible to determine the values of the pressure drops Δp_i in the working chambers of the machine. Moreover, in research systems, motor tests are most often carried out assuming a constant pressure drop Δp in the motor. This is mainly for practical reasons, as it is simply easier to set and control a constant pressure drop Δp in the hydraulic motor than a constant load (torque M) on the motor shaft. With this assumption, i.e. for Δp = const., a lower value of the torque M is observed, i.e.:

$$M = \frac{q_r \cdot \Delta p}{2 \cdot \pi} - M_{MpL} \quad (6)$$

where M_{MpL} are the mechanical-pressure losses. Publication [34] shows the influence of construction parameters and liquid parameters (the kinematic viscosity ν and the density ρ) on these losses.

The third type of losses occurring in a positive displacement machine are pressure losses Δp_{ich} in the internal channels of this machine. This refers to the pressure drop between the inlet connection and the working chamber being filled and between the working chamber being emptied and the outlet connection. As a result of pressure losses Δp_{ich} in the internal channels, a greater pressure drop Δp is observed in the motor, i.e. [44]:

$$\Delta p = \Delta p_i + \Delta p_{ich} \quad (7)$$

The pressure drop Δp_{ich} in the internal channels of the motor can be described by the following formula [44]:

$$\Delta p_{ich} = A \cdot Q^2 + B \cdot Q \quad (8)$$

If it is possible to determine the pressure losses Δp_{ich} in the internal channels, for example according to the methods described in [44], the mechanical losses M_L in the motor can be calculated using the formula:

$$M_L = M_{MpL} - \frac{q_r \cdot \Delta p_{ich}}{2 \cdot \pi} \quad (9)$$

It is worth emphasising that both the volumetric losses Q_L and the mechanical losses M_L are influenced by the actual working volume of the motor q_r. The relationship between the actual working volume q_r and the theoretical working volume q_t is described by formula (3). The theoretical working volume q_t does not have to be equal to the geometric working volume q_g, i.e. the volume calculated based on the technical documentation of the motor [39,42]. In publications [40–42], it was shown that incorrectly determined theoretical working volume q_t and actual working volume q_r result in incorrectly calculated losses, and consequently incorrectly calculated volumetric and mechanical efficiency of the motor. It may even happen that one of these efficiencies will have a value greater than one (which is, of course, nonsense).

On a test stand, as described below, it is often easier and more convenient to conduct tests of the motor as a function of its rotational speed n and with a constant pressure drop Δp. In this way, the characteristics of the absorbency Q of the motor are obtained as a function of its rotational speed n at various constant values of the pressure drop Δp in the motor. With such data, the theoretical working volume q_t of the motor can be determined using the method described in [40]. In brief, this volume can be expressed as:

$$q_t = \lim_{n \to \infty} \left(\lim_{\Delta p_i \to 0} (q_e)_{(n=const.)} \right) \quad (10)$$

where q_e is the effective absorbency of the motor per one revolution of its shaft and is defined as [6,39–42]:

$$q_e = \frac{Q}{n} \quad (11)$$

Based on the characteristics $q_e = f(1/n)_{\Delta p = const}$ the actual working volume q_r can also be determined, because for a given pressure drop (Δp = const.) in the motor is [40]:

$$q_e = \frac{Q}{n} + q_r \quad (12)$$

The total efficiency η_c is independent of the theoretical and actual working volume of the positive displacement machine. For a hydraulic motor, the total efficiency is defined as [3,45–46]:

$$\eta_C = \frac{M \cdot \omega}{Q \cdot \Delta p} \tag{13}$$

where ω is the angular velocity of the motor shaft.

The total efficiency η_c can also be assessed based on the increase in liquid temperature Δt in the motor ports. It is well known that the rise in liquid temperature Δt results from energy losses in components and hydraulic circuits [6]. The total efficiency η_C of the motor can be calculated using the following formula [17]:

$$\eta_c = 1 - \rho \cdot c \cdot \left(k + \frac{\Delta t}{\Delta p}\right) \tag{14}$$

where:

- ρ – the density of the liquid;
- c – the specific heat of the liquid;
- k – the constant.

The constant k depends on the initial temperature of the liquid. For example, for mineral oil at $t_1 = 40 \div 50$ °C is k = 0.128 °C/MPa [6] and for rapeseed oil k = 0.071 °C/MPa [17]. However, for water the value of this constant is not known. Therefore, the constant k for water will be the subject of this article.

The satellite motor described in this article was tested with two different liquids: edible refined rapeseed oil and pure tap water. These liquids differ significantly in viscosity and density (Fig. 3 and Fig. 4). Therefore, it is also expected that the losses in the motor supplied with these liquids will differ significantly. To quantitatively compare these losses, it is useful to define the following constants:

a) for the comparison of the volumetric losses Q_L:

$$X_{QL} = \frac{Q_{L(water)}}{Q_{L(oil)}} \tag{15}$$

b) for the comparison of the mechanical-pressure losses M_{MpL}:

$$X_{MpL} = \frac{M_{MpL(water)}}{M_{MpL(oil)}} \tag{16}$$

c) for the comparison of the pressure losses Δpich:

$$X_{pL} = \frac{\Delta p_{ich(water)}}{\Delta p_{ich(oil)}} \tag{17}$$

d) for the comparison of the mechanical losses M_L:

$$X_{ML} = \frac{M_{ML(water)}}{M_{ML(oil)}} \tag{18}$$

4. Working liquid

The following were used as working liquids in the hydraulic system:

1) refined rapeseed oil (edible oil);
2) pure tap water.

The dynamic viscosity μ characteristics of these liquids are shown in Fig. 3. The density ρ characteristics are shown in Fig. 4.

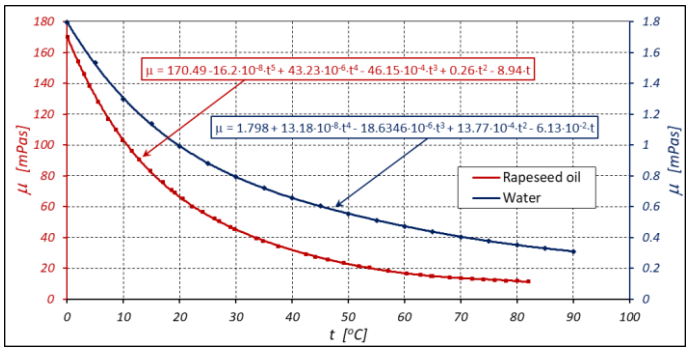

Figure 3. Dynamic viscosity μ of rapeseed oil and water.

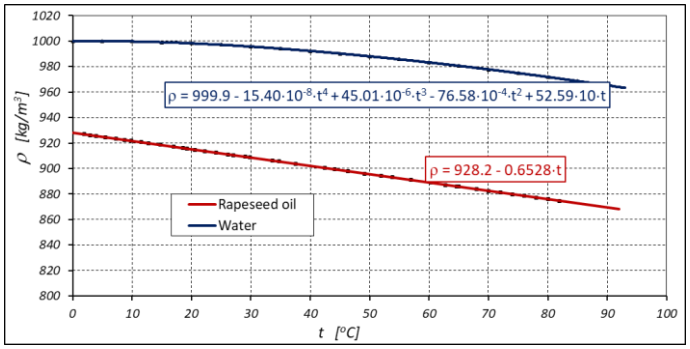

Figure 4. Density ρ of rapeseed oil and water.

The specific heat c of water is more than twice that of rapeseed oil. Due to the fact that rapeseed is cultivated in various regions of the world, the specific heat of different rapeseed oils may vary. According to [45], the specific heat c of rapeseed oil is $c = 1850 \frac{J}{kg \cdot K}$, while according to [47–48] it is $c = 2430 \frac{J}{kg \cdot K}$. For comparison, for water $c = 4180 \frac{J}{kg \cdot K}$ [45].

Water has poorer lubricating properties than rapeseed oil. The limit seizure pressure p_{oz} for refined rapeseed oil is p_{oz} = 287.5 MPa and for water p_{oz} = 255 MPa [18]. Therefore, the relative difference in the seizure pressure limit values is 11.3%.

5. Test stand

All experiments were conducted on the test rig shown in Fig. 5 and Fig. 6. This test rig has been described in several publications, particularly in [17]. It is an energy-efficient system,

known as a circulating power system. The stand enables testing of both the pump and the hydraulic motor within a rotational speed range of 30 to 2000 rpm and a working pressure of up to 25 MPa.

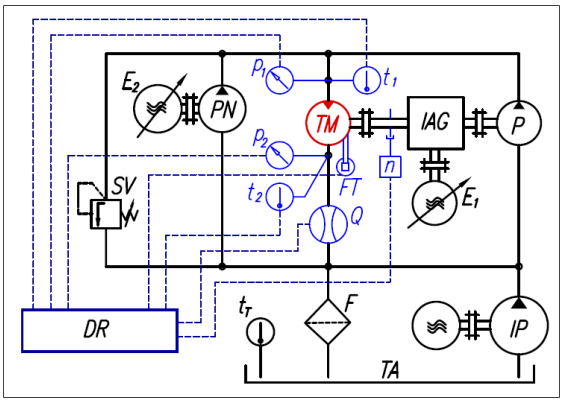

Figure 5. The hydraulic and measuring system of the test rig: P – pump, TM – tested motor, PN – pump for filling leaks in P and M, IP – impeller pump, SV – safety valve, F – filter, TA – tank, IAG – intersecting axis gear, E_1 and E_2 – electric motors with frequency converters, DR – data recorder, p_1, p_2 – pressure transducers, t_1, t_2, tT – temperature transducers, Q – flowmeter, FT – force transducer (measurement of the torque M), n – inductive sensor (measurement of the rotational speed n) [17].

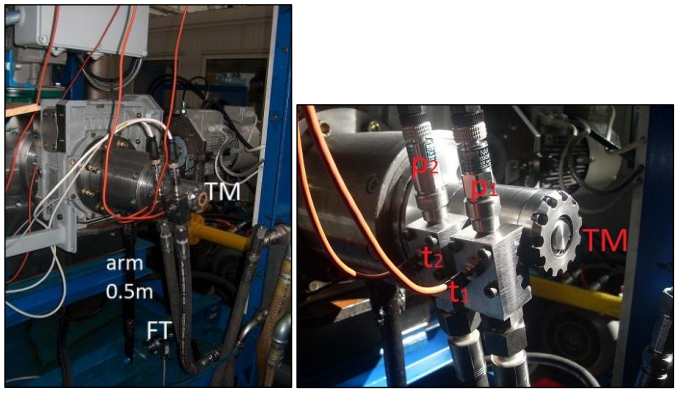

Figure 6. Tested satellite motor on the test stand: TM – tested motor, p_1 and p_2 – pressure transducers, t_1 and t_2 – RTD temperature sensors, FT – force transducer.

Table 1. Measured parameters and data of measuring instruments.

Measured parameter		Measuring instrument	Range	Class
Pressure	p_1 p_2	strain gauge pressure transducer	0÷25 MPa 0÷2.5 MPa	0.3
Flow rate	Q	mass flowmeter	0÷33 l/min	0.1
Torque	M	strain gauge force transducer FT (on the arm 0.5m length)	0÷100 Nm	0.1
Rotational speed	n	inductive sensor	± 0.01 rpm	
Temperature	t_1	RTD temperature sensor	-20÷150 °C	A

The parameters measured on the test stand are listed in Table 1. During testing, the adjustable and therefore easily controllable parameters are the pressure p_1 at the supply port of the tested motor and the rotational speed n of the motor shaft. The resulting parameters are the torque M on the motor shaft and the motor's absorbency Q.

6. Results of research

Two types of motor tests were performed, using both rapeseed oil and water as working liquids, i.e.:

1) short-term tests (basic tests);
2) durability tests.

The tests were conducted using two satellite mechanisms. The first mechanism was initially used for short-term tests, followed by durability tests with water as the working liquid. The second mechanism was used in the same way, but for tests with rapeseed oil. Before testing, both mechanisms (i.e., the new mechanisms) had identical axial clearances of the satellites and rotor (Fig. 7), i.e.:

- the height of the curvature $H_E = 20 \pm 0.005$ mm;
- the axial clearance of the rotor $h_R = 4.5$ µm;
- the axial clearance of the satellites $h_S = 6.2$ µm.

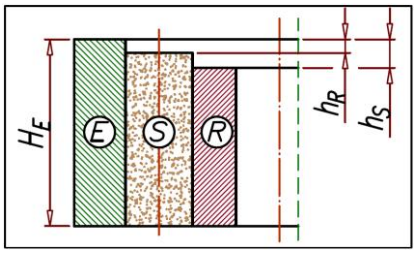

Figure 7. The axial clearances of the rotor and the satellite: E – curvature, R – rotor, S – satellite, H_E – height of the curvature, h_S – the axial clearance of the satellite, h_R – the axial clearance of the rotor.

The liquid temperature was stabilised only during the short test. During the durability test, the liquid temperature was not stabilised. In this way, the test conditions reflected the actual motor operating conditions in an industrial device.

In the remainder of this article, physical and technical quantities are expressed in units such as those in Table 1. These are not strictly SI units. Therefore, in order to easily convert (if necessary) test results to strict SI units, please note that:

- 1 lpm = 1/60000 m^3/s,
- 1 rpm = 1/60 rps,
- 1 cm^3/rev = 10^{-6} m3/rev,

– 1 MPa = 10^6 Pa and 1 bar = 10^5 Pa,
– 1 °C = (1 + 273.15) K.

6.1. Short-term tests (basic tests) results

The short-term tests aimed to record basic motor parameters and determine the characteristics of absorbency Q, torque M, volumetric and mechanical losses, as well as to determine the theoretical and actual working volume of the motor.

The tests were conducted within the motor speed range n from 30 to 1500 rpm and within the pressure drop range Δp in the motor from 1 to 25 MPa. During the tests, the fluid temperature was stabilised at 40±2 °C, which corresponds to:

a) the dynamic viscosity of water μ = 0.658 mPa·s (the kinematic viscosity ν = 0.66 cSt);
b) the dynamic viscosity of rapeseed oil μ = 32 mPa·s (the kinematic viscosity ν = 44 cSt).

The results recorded during the tests allowed the characteristics of the motor's absorbency Q and the torque M on the motor shaft to be plotted (Fig. 8, Fig. 9, Fig. 10 and Fig. 11).

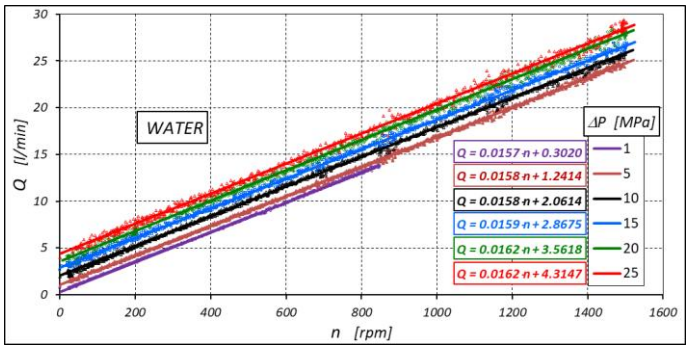

Figure 8. Characteristics of the absorbency Q of the motor as a function of the rotational speed n at different constant pressure drops Δp in the motor. Working liquid: WATER.

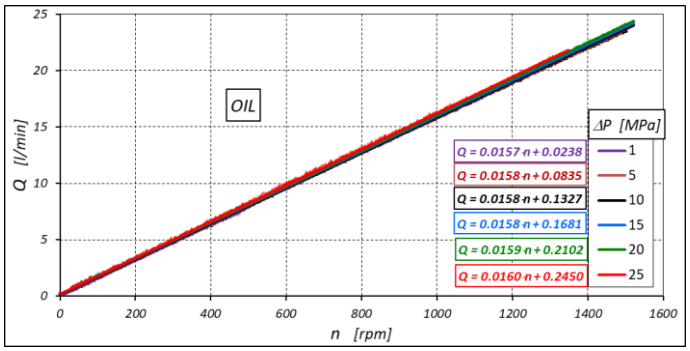

Figure 9. Characteristics of the absorbency Q of the motor as a function of the rotational speed n at different constant pressure drops Δp in the motor. Working liquid: RAPESEED OIL.

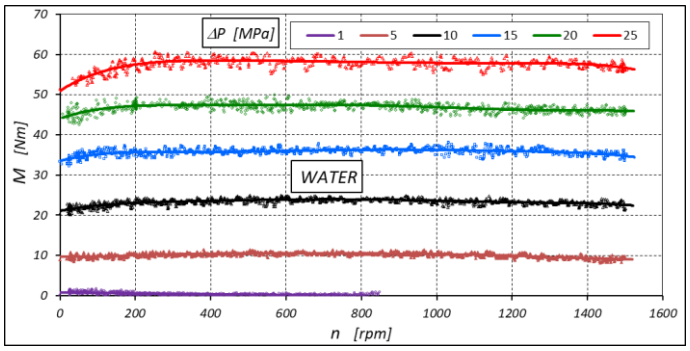

Figure 10. Characteristics of the torque M on the motor shaft as a function of the rotational speed n at different constant pressure drops Δp in the motor. Working liquid: WATER.

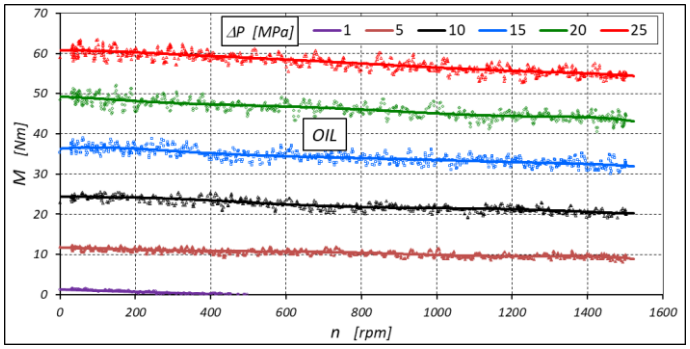

Figure 11. Characteristics of the torque M on the motor shaft as a function of the rotational speed n at different constant pressure drops Δp in the motor. Working liquid: RAPESEED OIL.

The results for the motor's absorbency Q are required to calculate the effective absorbency qe (according to formula (11)). The characteristics of the effective absorbency qe of the motor supplied with water and rapeseed oil are shown in Fig. 12 and Fig. 13.

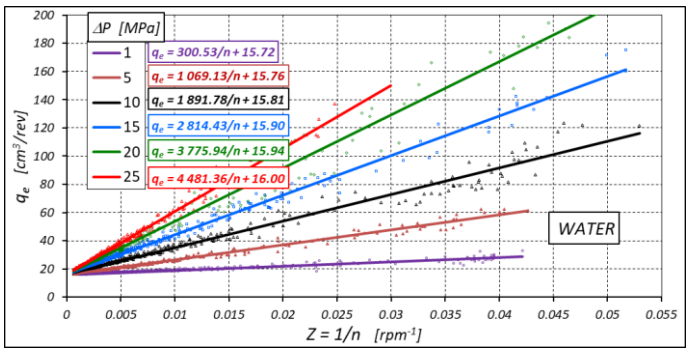

Figure 12. Characteristics of the effective absorbency q_e of the motor at different constant pressure drops Δp in the motor. Working liquid: WATER.

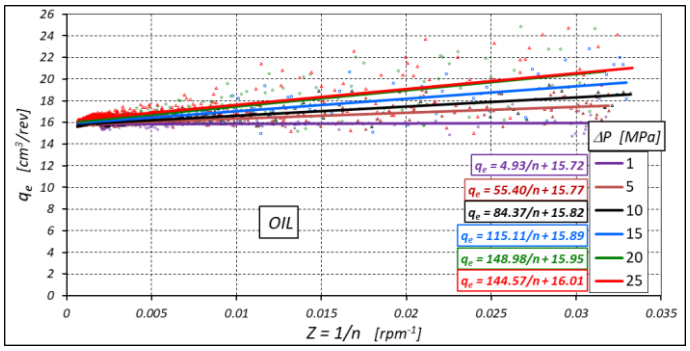

Figure 13. Characteristics of the effective absorbency qe of the motor at different constant pressure drops Δp in the motor. Working liquid: RAPESEED OIL.

Based on the mathematical equations (such as formula (12)) describing the characteristics shown in Fig. 12 and Fig. 13, the characteristics of the actual working volume q_r of the motor supplied with both liquids were determined (Fig. 14).

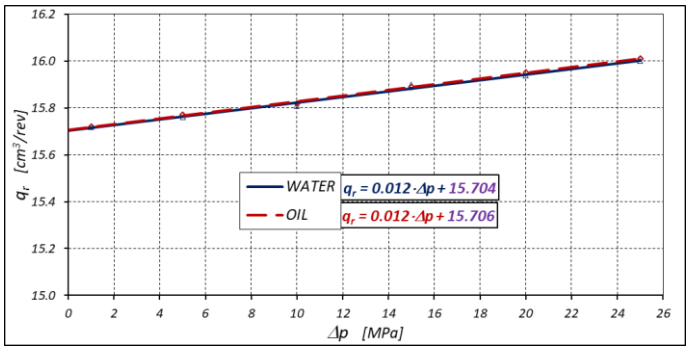

Figure 14. Characteristics of the actual working volume qr of the motor as a function of pressure drop Δp in the motor. Working liquids: WATER and RAPESEED OIL.

The characteristics shown in Fig. 14 indicate that the actual working volume q_r of the motor, whether supplied with water or rapeseed oil, is practically the same. This confirms that the type of liquid does not affect the actual and theoretical working volume. The experimental results further confirm that the actual working volume q_r can be described by formula (3). For the tested motor:

$$q_r = 0.012 \cdot \Delta p + 15.705 \qquad (19)$$

In the above formula, Δp is in [MPa] and q_r is in [cm³/rev]. From this formula it follows that the theoretical working volume of the motor is q_t = 15.705 cm³/rev.

Knowledge of the actual working volume q_r of the motor allows calculation (after transforming formula (1)) and plotting of the characteristics of volumetric losses Q_L (Fig. 15).

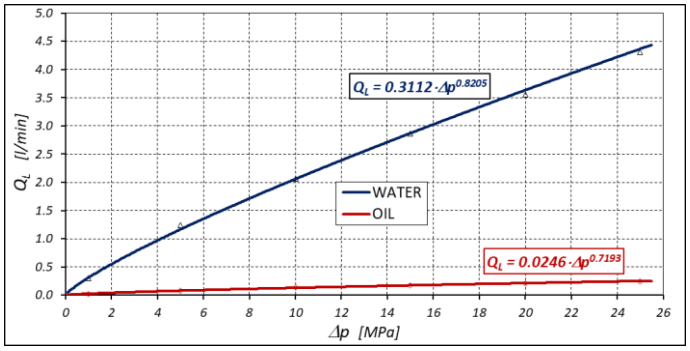

Figure 15. Characteristics of volumetric losses Q_L in the motor as a function of pressure drop Δp in the motor. Working liquids: WATER and RAPESEED OIL.

Knowledge of the actual working volume q_r of the motor allows calculation (according to formula (6)) and plotting of the characteristics of mechanical-pressure losses M_{MpL} (Fig. 16 and Fig. 17).

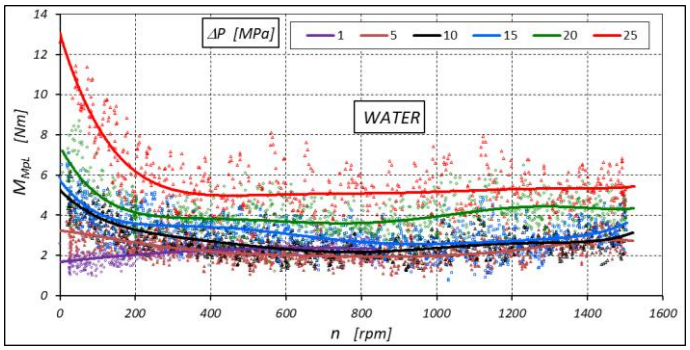

Figure 16. Characteristics of mechanical-pressure losses M_{MpL} in the motor as a function of rotational speed n at different constant pressure drops Δp in the motor. Working liquid: WATER.

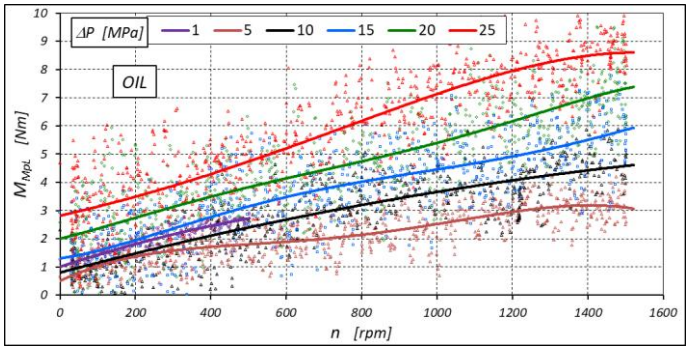

Figure 17. Characteristics of mechanical-pressure losses M_{MpL} in the motor as a function of rotational speed n at different constant pressure drops Δp in the motor. Working liquid: RAPESEED OIL.

The pressure drop Δp_{ich} in the internal channels of the motor was determined according to the method described in

publication [44]. The pressure drop characteristics in the internal channels of the motor supplied with water and rapeseed oil are shown in Fig. 18.

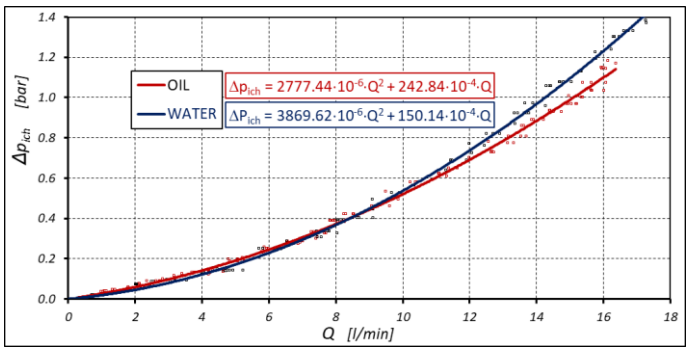

Figure 18. Characteristics of pressure drop Δp_{ich} in the internal channels of the motor as a function of motor absorbency Q. Working liquids: WATER and RAPESEED OIL.

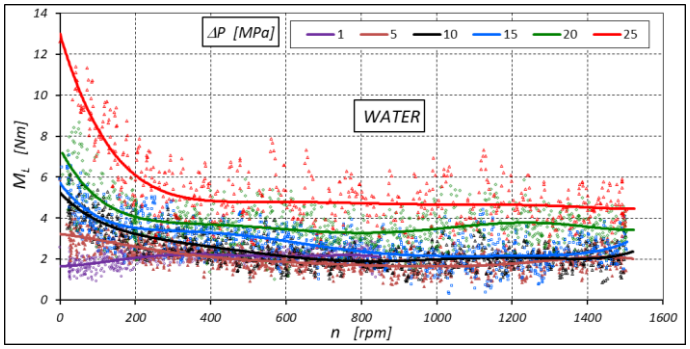

Figure 19. Characteristics of mechanical-pressure losses MMpL in the motor as a function of rotational speed n at different constant pressure drops Δp in the motor. Working liquid: WATER.

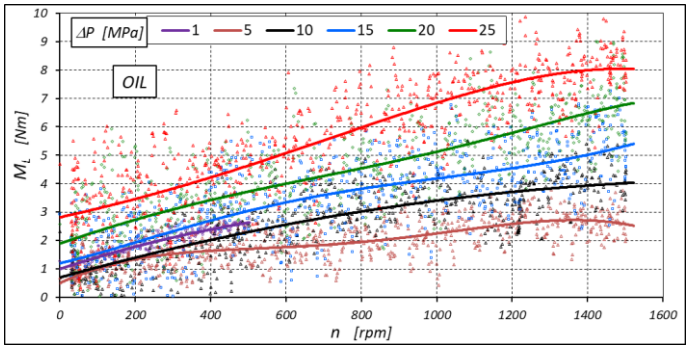

Figure 20. Characteristics of mechanical losses M_{ML} in the motor as a function of rotational speed n at different pressure constant drops Δp in the motor. Working liquid: RAPESEED OIL.

Having determined the pressure drops Δp_{ich} in the internal channels of the motor and the mechanical-pressure losses M_{MpL}, it is possible to determine the mechanical losses M_L in the motor (use formula (9), substituting formula (8) and formula (1) into it). The characteristics of mechanical losses M_L in the motor supplied with water and rapeseed oil are shown in Fig. 19 and Fig. 20, respectively.

7. Durability tests results

The durability tests of the satellite motor were conducted after the short-term tests, using the same satellite mechanisms as in the short-term tests.

The experimental data relating to the setup time τ_s, that is the time required to start and stop the hydraulic and measurement systems, set the parameters, etc., are not included in the test results (tables and figures). During this period, the motor operated at speeds in the range 0÷1500 rpm and at a pressure drop Δp corresponding to each measurement series, i.e. up to Δp = 20 MPa. It was estimated that the duration of motor operation with different parameters was about 40 minutes. The mean rotational speed during this period was approximately n_m = 750 rpm.

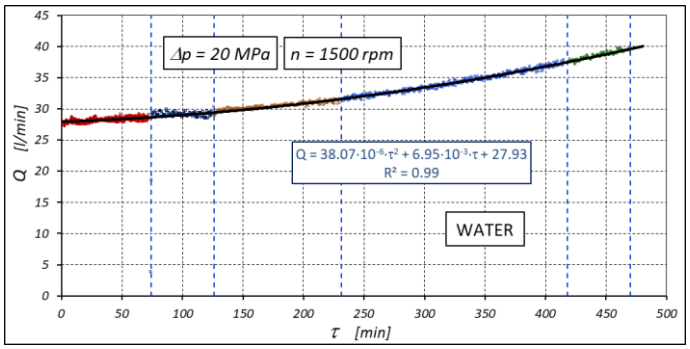

Figure 21. Characteristics of the motor absorbency Q as a function of time τ. Working liquid: WATER.

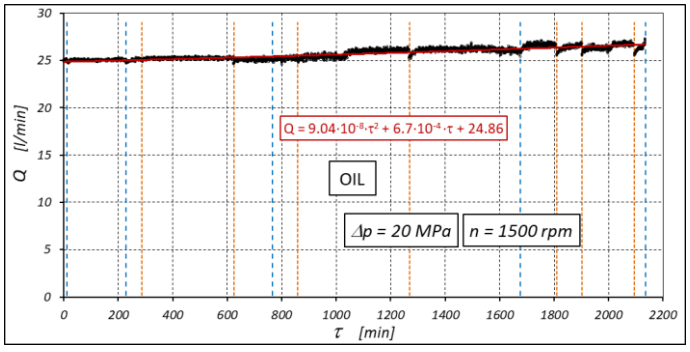

Figure 22. Characteristics of the motor absorbency Q as a function of time τ. Working liquid: RAPESEED OIL [17].

The durability tests of the motor, supplied with both water and rapeseed oil, were carried out at a constant pressure drop Δp = 20±0.5 MPa and a constant motor shaft speed n = 1500±1 rpm.

As a result, the characteristics of the motor absorbency Q (Fig. 21 and Fig. 22) and the characteristics of the torque M on the motor shaft (Fig. 23 and Fig. 24) were recorded as functions of time τ. Fluid temperatures at the motor ports were also recorded (Fig. 25 and Fig. 26). Fluid temperature was not stabilised during the tests, to reflect the conditions prevailing in an actual hydraulic system. The motor tests were periodically interrupted and the motor was disassembled. During this time, visual inspections and mass measurements of the working mechanism components were performed. The duration of the test breaks is marked on the graphs with vertical dashed straight lines.

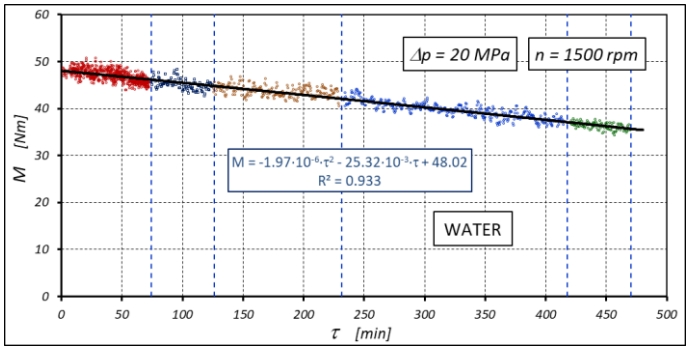

Figure 23. Characteristics of the torque M as a function of time τ. Working liquid: WATER.

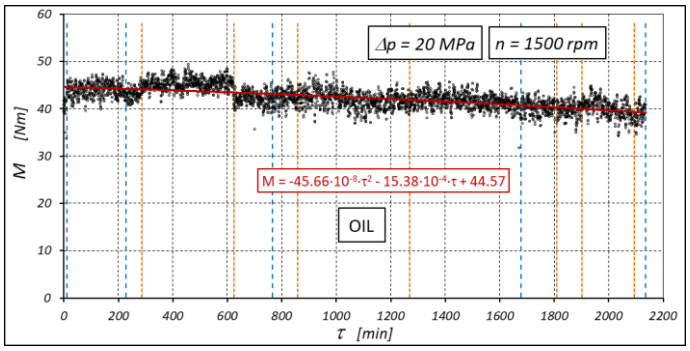

Figure 24. Characteristics of the torque M as a function of time τ. Working liquid: RAPESEED OIL [17].

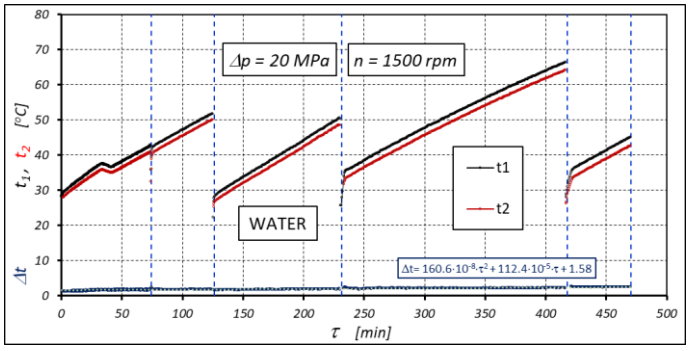

Figure 25. Characteristics of the temperatures t_1 and t_2 in the motor ports as a function of time τ. Working liquid: WATER.

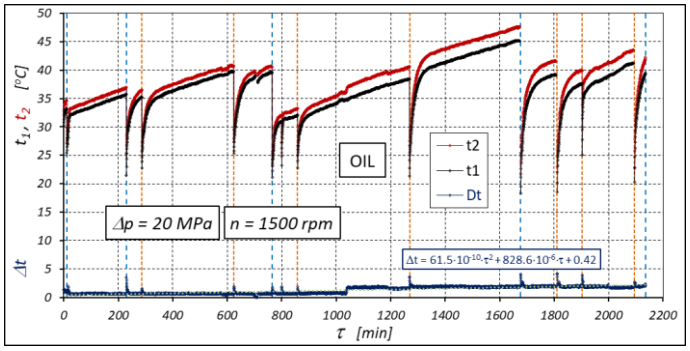

Figure 26. Characteristics of the temperatures t_1 and t_2 in the motor ports as a function of time τ. Working liquid: RAPESEED OIL [17].

Characteristics of volumetric losses Q_L in the motor supplied with rapeseed oil and water are shown in Fig. 27. Fig. 28 presents the characteristics of mechanical-pressure losses M_{MpL}.

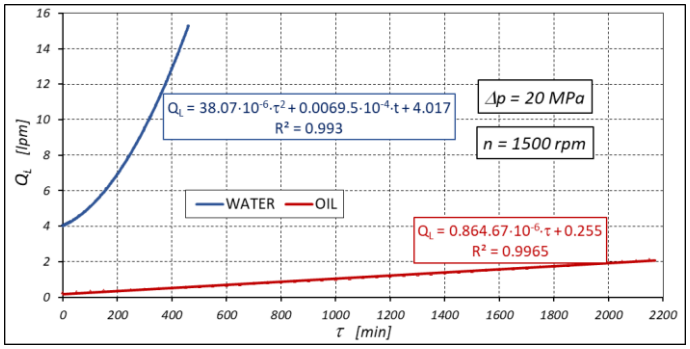

Figure 27. Characteristics of volumetric losses Q_L in the motor as a function of time τ. Working liquid: WATER and RAPESEED OIL.

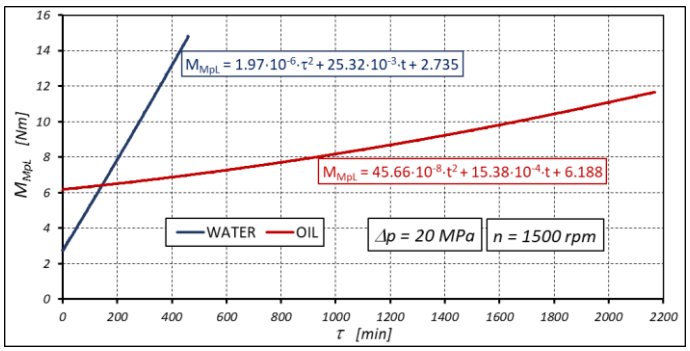

Figure 28. Characteristics of mechanical-pressure losses M_{MpL} in the motor as a function of time τ. Working liquid: WATER and RAPESEED OIL.

Having the characteristics of mechanical-pressure losses M_{MpL} and the characteristics of pressure losses Δp_{ich} in the internal channels of the motor, the mechanical losses M_L in the motor can be calculated according to formula (9). The characteristics of these losses are shown in Fig. 29.

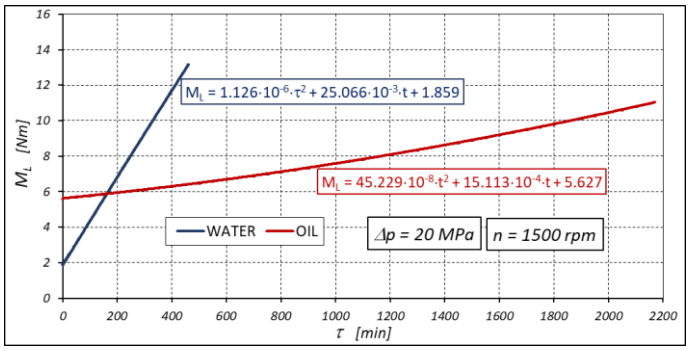

Figure 29. Characteristics of mechanical losses M_L in the motor as a function of time τ. Working liquid: WATER and RAPESEED OIL.

Based on the experimental data, the characteristics of the total efficiency η_C of the motor were determined using formula (13) (Fig. 30).

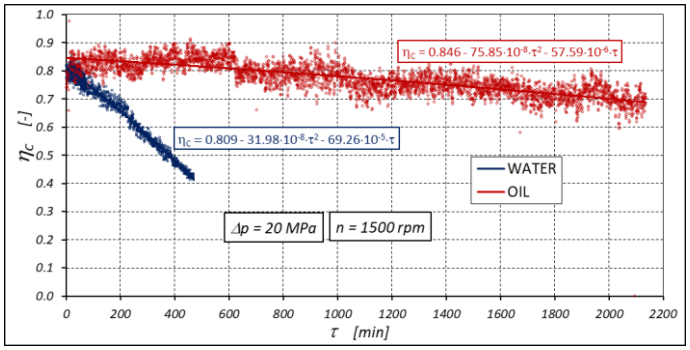

Figure 30. Characteristics of total efficiency η_C of the motor as a function of time τ. Working liquid: WATER and RAPESEED OIL.

As mentioned above, during the tests, the engine was disassembled and the height and weight of its components were inspected and measured. Table 2 and Table 3 provide the following data:

- m_S – the average mass of all satellites;
- m_E – the mass of the curvature;
- m_R – the mass of the rotor;
- H_E – the height of the curvature (Fig. 7);
- h_R – the axial clearance of the rotor and satellite (Fig. 7);
- h_S – the average axial clearances of all satellites (Fig. 7).

The satellite mechanism of the tested motor was destroyed (Fig. 31):

- with water – after 482 minutes of operation;
- with rapeseed oil – after 2135 minutes of operation.

Table 2. Mass, height and clearances of the components of the satellite mechanism – test for Δp = 20 MPa. Symbols H_E, h_R and h_S like in Fig. 7. Working liquid: RAPESEED OIL [17].

		m_E [g]	m_R [g]	m_S [g]	H_E [mm]	h_R [μm]	h_S [μm]
Time τ [min]	0	99.813	43.104	4.536	19.998	4.5	6.2
	11.5	99.801	43.103	4.535	20.007	6.5	6.45
	229	99.788	43.075	4.533	20.009	7.0	7.1
	765	99.781	43.010	4.529	20.011	7.0	9.1
	1677	99.741	42.745	4.521	20.010	7.5	8.35
	2135	99.726	damage	4.516*	20.019	damage	7.75*

* measurement only for four satellites (6 were broken)

Table 3. Mass, height and clearances of the components of the satellite mechanism – test for Δp = 20 MPa. Symbols H_E, h_R and h_S like in Fig. 7. Working liquid: WATER.

		m_E [g]	m_R [g]	m_S [g]	H_E [mm]	h_R [μm]	h_S [μm]
Time τ [min]	0	99.293	43.168	4.549	19.989	4.6	6.3
	146.5	99.213	43.048	4.531	19.995	5.1	6.6
	250	98.785	42.548	4.465	20.000	5.6	10.1
	433	98.293	42.242	4.406	19.998	5.7	15.1
	482.2	98.094	41.895	4.364	20.001	damage	damage

Figure 31. View of the destroyed satellite mechanism. Left: WATER, right: RAPESEED OIL.

8. Discussion

8.1. Short-term tests (basic tests)

Based on the results of the short-term motor tests, it was found that the type of working liquid does not affect the theoretical working volume q_t and the actual working volume q_e of the motor (Fig. 14 and formula (19)). This confirms the correctness of the method for determining these volumes described in the publication [40].

The experimental results (Fig. 15) allow the conclusion that the following empirical formula can describe volumetric losses in the motor:

a) supplied with oil:

$$Q_{L(oil)} = 0.0246 \cdot \Delta p^{0.7193} \quad (20)$$

b) supplied with water:

$$Q_{L(water)} = 0.3112 \cdot \Delta p^{0.8205} \quad (21)$$

In the above formulas ((20) and (21)) Δp is in [MPa], and $Q_{L(oil)}$ and $Q_{L(water)}$ are in [l/min].

The ratio X_{QL} of volumetric losses in the motor supplied with water and rapeseed oil, calculated according to formula (15), can be described by the following empirical formula (Fig. 32):

$$X_{QL} = 12.636 \cdot \Delta p^{0.1012} \tag{22}$$

where Δp is in [MPa]. This formula is valid for the above-mentioned viscosities and densities of the liquid and for Δp > 0. It is clear that for Δp = 0 is $Q_L = 0$, regardless of the type of liquid.

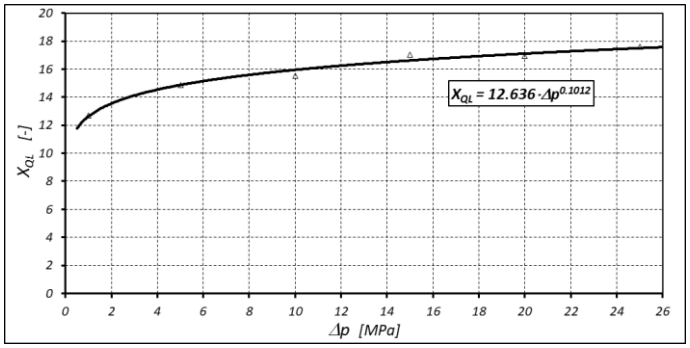

Figure 32. Characteristics of the volumetric losses ratio X_{QL} in the motor supplied with water and rapeseed oil as a function of the pressure drop Δp in the motor.

From Fig. 32, it can be seen that in the motor supplied with water, the volumetric losses are several times greater than in the motor supplied with rapeseed oil. In the motor supplied with water, higher mechanical-pressure losses M_{MpL} are observed (Fig. 16 and Fig. 17). The ratio of mechanical-pressure losses X_{MpL}, calculated according to formula (16), is shown in Fig. 33.

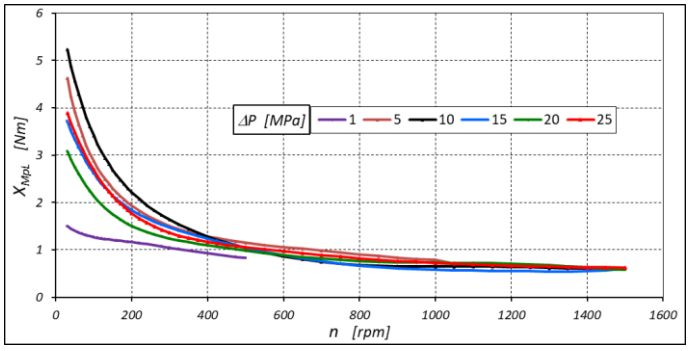

Figure 33. Characteristics of the mechanical-pressure losses ratio X_{MpL} in the motor supplied with water and rapeseed oil as a function of rotational speed n at various constant pressure drops Δp in the motor.

The characteristics shown in Fig. 33 are proposed to be described by an empirical formula in the following form:

$$X_{MpL} = \frac{12000}{8000 \cdot \Delta p^{-0,63} + (\ln(n))^5} \tag{23}$$

where:

– Δp – the pressure drop in the motor in [MPa];

– n – the rotational speed of the motor shaft in [rpm].

The above formula describes the ratio of mechanical losses in the motor supplied with water and rapeseed oil. As can be seen, the ratio of these losses is a function of both the rotational speed of the motor shaft and the pressure drop in the motor. Presented formula (23) is valid for Δp > 0 and n > 0 and enables estimation of the value of mechanical-pressure losses M_{MpL} in the motor supplied with water based on the results of tests on this motor supplied with rapeseed oil, i.e. without the need to carry out tests of the motor supplied with water.

The results of the experiment also showed the effect of the type of liquid on the pressure drop Δp_{ich} in the internal channels of the motor (Fig. 18). The ratio X_{pL} of pressure losses Δp_{ich} in the internal channels of the motor supplied with water and supplied with rapeseed oil, calculated according to formula (17), is shown in Fig. 34.

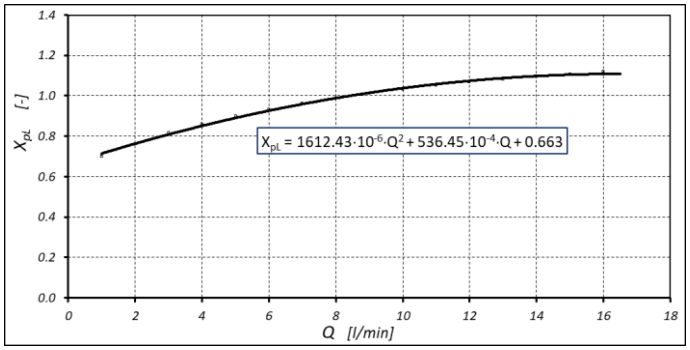

Figure 34. Characteristics of the pressure losses ratio X_{pL} in the motor supplied with water and rapeseed oil as a function of the motor absorbency Q.

The ratio X_{pL} of pressure losses Δp_{ich} in the internal channels of the motor can be described by the empirical formula in the following form:

$$X_{pL} = 1612.43 \cdot 10^{-6} \cdot Q^2 + 536.45 \cdot 10^{-4} \cdot Q + 0.633 \tag{24}$$

where Q is in [lpm]. This formula is valid for Q > 1 lpm. For smaller absorbency Q the minimum value of X_{pL} depends on the viscosities of the liquids, that is:

$$X_{pL} = \frac{\mu_W}{\mu_O} = min. \tag{25}$$

where μ_W is the dynamic viscosity of water and μ_O is the dynamic viscosity of rapeseed oil. For the case under consideration is $X_{pL} = 0.02$.

Knowledge of the pressure drop characteristics in the internal channels of the motor enables the determination of the mechanical losses characteristics in this motor (Fig. 19 and Fig. 20). The ratio of mechanical losses X_{ML} in the motor supplied with water and supplied with rapeseed oil, calculated according to formula (18), is shown in Fig. 35.

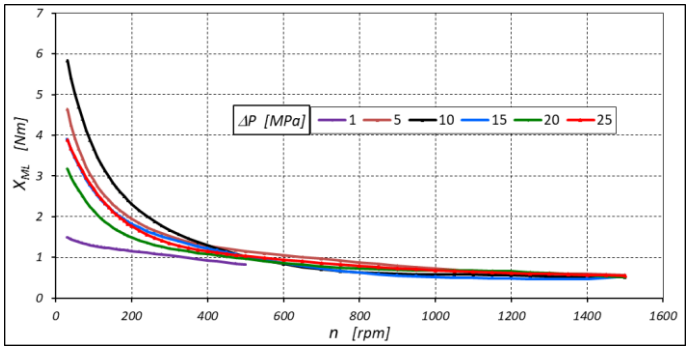

Figure 35. Characteristics of the mechanical losses ratio X_{ML} in the motor supplied with water and rapeseed oil as a function of rotational speed n at various constant pressure drops Δp in the motor.

The characteristics shown in Fig. 35 indicate that, in the range of the motor shaft speeds up to approximately 500 rpm, mechanical losses M_L in the motor supplied with water are greater than those in the motor supplied with rapeseed oil. Above this speed, the opposite trend is observed: mechanical losses M_L in the motor supplied with water are lower than those in the motor supplied with oil. The cause of this phenomenon has not yet been thoroughly investigated and explained. In publication [34], it was indicated that there is a component of mechanical losses in the satellite motor resulting from the compression of liquid in the dead chambers of the satellite mechanism (chambers $V_{ch\text{-}min}$ and $V_{ch\text{-}max}$ in Fig. 2) and the compression of liquid from the inter-tooth spaces of the cooperating elements of the satellite mechanism. Therefore, it can be assumed that at high rates of change in the volume of enclosed spaces (here above 500 rpm), pumping water from these spaces through the gaps requires a much smaller increase in pressure. The fluid parameter with significant impact here is dynamic viscosity μ. This explains the lower mechanical losses M_L in a motor supplied with water at n > 500 rpm. The observed phenomenon will be thoroughly investigated in the future, and the hypothesis will be confirmed or rejected.

8.2. Durability tests

Experimental results have shown that the durability of the satellite mechanism under high load conditions corresponding to a pressure drop of Δp = 20 MPa in the motor is very short. For the motor supplied with rapeseed oil, this durability is only 35.5 hours (Table 2), while for the motor supplied with water, it is only 8 hours (Table 3). Therefore, the durability of the motor supplied with water is more than 4.4 times shorter than that of the same motor supplied with rapeseed oil. It can be concluded that, for the satellite motor, a pressure drop of 20 MPa is too high. Article [17] indicates that in the case of the motor being supplied with rapeseed oil, to achieve satisfactory durability of the satellite mechanism, the motor should be operated at Δp < 10 MPa. It can be assumed that in the case of the motor supplied with water this pressure drop should be even lower.

During the operation of the motor, whether supplied with water or rapeseed oil, wear occurs on the working mechanism components. This is primarily manifested by a loss of weight of these components (Table 2 and Table 3).

Publication [37] describes the mechanism of wear of the satellite mechanism components. It was indicated, among other things, that the wear of the rotor teeth occurs faster than the wear of the curvature teeth. This is because the number of loads on each rotor tooth per revolution of the rotor is greater than the number of loads on the curvature teeth. Furthermore, due to centrifugal force, the satellite is pressed against the curvature, which increases the clearances between the mating teeth of the satellite and the rotor [17]. These increased clearances also significantly affect the wear of the satellite teeth, especially in a water environment (Fig. 38).

To objectively compare the amount of wear of components, publication [17] defined the concept of the relative weight loss of the components:

$$\delta m_X = 100 \cdot \left(1 - \frac{m_X}{m_{X(t=0)}}\right) \tag{26}$$

where:

- $m_{X(t=0)}$ – the initial mass of the element for t = 0 min. (X = S for satellites, X = R for the rotor and X = E for the curvature);
- m_X – the mass of the element during the test.

Characteristics of the relative weight loss of the components (plotted using data from Table 2 and Table 3) are shown in Fig. 36, Fig. 37 and Fig. 38. The characteristics of rapeseed oil were taken from publication [17].

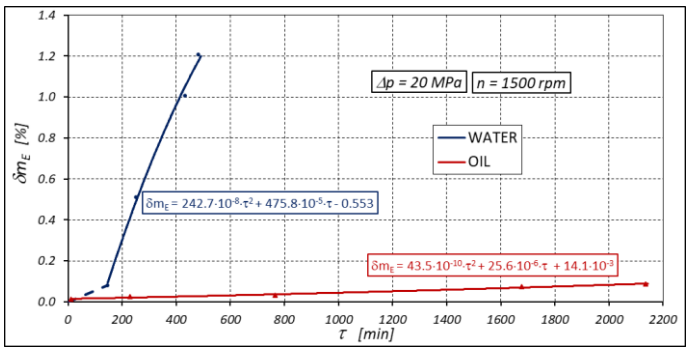

Figure 36. Percentage loss δm_E of the curvature mass as a function of time τ. Working liquids: WATER and RAPESEED OIL.

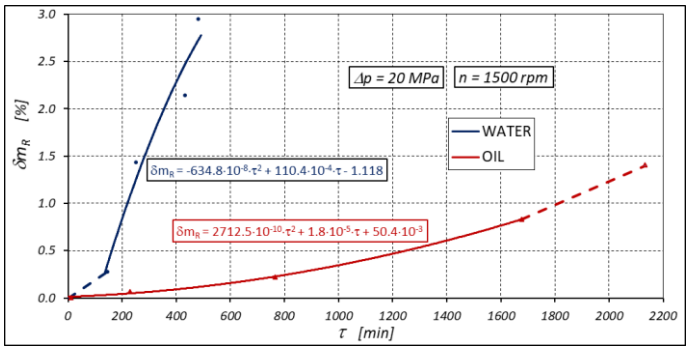

Figure 37. Percentage loss δm_R of the rotor mass as a function of time τ. Working liquids: WATER and RAPESEED OIL.

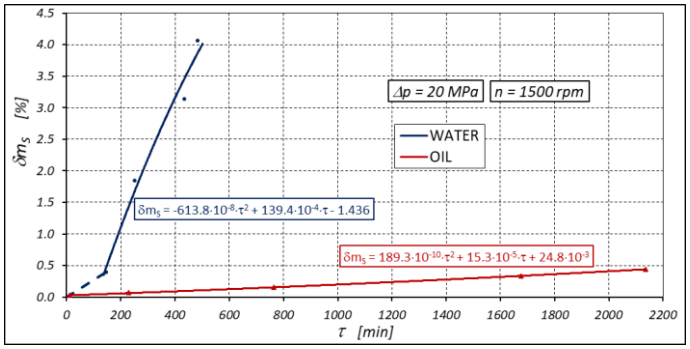

Figure 38. Percentage loss δm_S of the satellites mass as a function of time τ. Working liquids: WATER and RAPESEED OIL.

According to Fig. 30, the total efficiency η_C of the satellite motor changes over the course (time τ in [min]) of its operation as follows:

a) for water:

$$\eta_C = 0.809 - 31.99 \cdot 10^{-8} \cdot \tau^2 - 69.26 \cdot 10^{-5} \cdot \tau \qquad (27)$$

b) for rapeseed oil:

$$\eta_C = 0.846 - 75.85 \cdot 10^{-8} \cdot \tau^2 - 57.59 \cdot 10^{-6} \cdot \tau \qquad (28)$$

A decrease in the total efficiency η_C of the motor during operation is reflected in an increase in the temperature Δt of the liquid in the motor (measured at the motor ports) (Fig. 25 and Fig. 26). Publication [17] demonstrated that this Δt is the result of energy losses occurring in the motor. Thus, for the motor:

a) supplied with water:

$$\Delta t = 1.58 + 160.6 \cdot 10^{-8} \cdot \tau^2 + 112.4 \cdot 10^{-5} \cdot \tau \qquad (29)$$

b) supplied with rapeseed oil:

$$\Delta t = 0.42 + 61.5 \cdot 10^{-10} \cdot \tau^2 + 828.6 \cdot 10^{-6} \cdot \tau \qquad (30)$$

In the above formulas ((29) and (30)) time τ is in [min]) and Δt is in [°C].

With the values of the total efficiency η_C of the motor (Fig. 30) and the temperature increase Δt in its connections available (Fig. 25), it is possible to estimate the value of the constant k by appropriately transforming formula (14). For the motor supplied with water, the calculated value of constant k is 0.023 °C/MPa. For comparison, for rapeseed oil k = 0.071 °C/MPa (as stated above).

The loss of mass of the working mechanism components (Table 2, Table 3) results mainly from wear of the teeth of this mechanism. This wear progresses most rapidly in the water environment (Fig. 36, Fig. 37 and Fig. 38). As wear increases, the inter-tooth clearances in the elements and the axial clearances in the satellites and rotor also increase. This leads to greater volumetric (Fig. 27) and mechanical losses (Fig. 29).

9. Final conclusion

The results of the satellite motor tests have shown that under high load conditions, the durability of the satellite mechanism is very low, regardless of whether the motor is supplied with water or rapeseed oil. According to publication [16], the satellite motor supplied with rapeseed oil would operate with a pressure drop Δp no greater than 10 MPa. Moreover, for reasons of durability, a water-powered motor should operate under low loads. In addition, the test results confirmed the theoretical analyses described in [37], which state that satellite mechanisms should operate at low rotational speeds.

To increase the durability of the satellite mechanism, it is necessary to seek other tooth profiles for this mechanism and steels that are more resistant to wear.

References

1. Kosucki A, Szczepaniak M, Skowrońska J, Grzejszczyk P, Stawiński Ł. Data-driven operational pressure estimation for hydraulic actuators fed by fixed displacement pump with variable speed. *Eksploatacja i Niezawodnosc – Maintenance and Reliability* 2025; 27(1). http://doi.org/10.17531/ein/192758.
2. Stawiński Ł, Kosucki A, Skowrońska J, Malenta P. Energy efficiency mmprovement of hydraulic indirect elevator. *Energies* 2025; 18(9): 2163. https://doi.org/10.3390/en18092163.
3. Stryczek S. *Napęd Hydrostatyczny*. WNT, Warszawa; 2005.
4. Collective work. *Hydraulics in industrial and mobile applications*. ASSOFLUID, Milano; 2007.
5. Yeaple F. *Fluid power design handbook*. CRC Press Taylor & Francis Group, New York; 1995.
6. Balawender A. *Analiza energetyczna i metodyka badań silników hydraulicznych wolnoobrotowych* (*Energy analysis and methodics of testing of low-speed hydraulic motors*). Scientific book of the Gdansk University of Technology, Mechanika No. 54. Gdansk University of Technology Publishing House, Gdansk; 1988.
7. PN-EN ISO 6743/4:2003 Standard. *Środki smarowe, oleje przemysłowe i produkty podobne*.
8. Xing T, Huang Y, Gao C, Ruan J. Characteristic study of a valve-matched flow single-piston miniature water-hydraulic pump. *IEEE Access* 2024; 12. https://ieeexplore.ieee.org/document/10630511 [accessed 12 January 2026]. doi: 10.1109/ACCESS.2024.3440197.
9. Todić N, Savić S, Gordić D, Petrović R. Experimental research of the hydrodynamic processes of an axial piston water hydraulic pump. *Machines* 2022; 10(9): 728. https://doi.org/10.3390/machines10090728.
10. Xing T, Huang Y, Gao C, Ruan J. Research on the output characteristic of a new water hydraulic electrohydraulic motor. *IEEE Access* 2023; 11. https://ieeexplore.ieee.org/document/10124942 [accessed 12 January 2026]. doi: 10.1109/ACCESS.2023.3276879.
11. Yang L., Wang G., Nie S.: Speed characteristics analysis and simulation of the water hydraulic axial piston motor. *World Journal of Engineering* 2016; 13(6): 524-528. https://doi.org/10.1108/WJE-09-2016-0086.
12. Rudko T, Rybczynski R. Właściwości smarne olejów roślinnych i mineralnych stosowanych w układach tnących pilarek (Lubrication properties of vegetable and mineral oils used for cutting mechanism of chainsaws). *Acta Agrophysica* 2010; 15(1): 145-153. http://www.acta-agrophysica.org/Lubrication-properties-of-vegetable-and-mineral-oils-used-for-cutting-mechanism-of,107286,0,2.html [accessed 09 January 2026].
13. Cieslikowski B, Slipek Z. Zmienność cech oleju rzepakowego w warunkach przechowywania (Variance of rape oil qualities under storage conditions). *Inżynieria Rolnicza* 2006; 13. https://ir.ptir.org/artykuly/pl/88/IR%2888%29_418_pl.pdf [accessed 09 January 2026].
14. Drabik J. Ocena odporności na utlenianie oraz właściwości smarnych kompozycji oleju roślinnego (The assessment of oxidation stability and of lubricating properties of vegetable oil compositions). Tribologia 2009; 3. https://t.tribologia.eu/resources/html/article/details?id=165245&language=pl [accessed 09 January 2026].
15. Rogos E, Urbanski A. Biodegradowalny olej hydrauliczny o podwyższonych właściwościach smarnych (Biodegradable hydraulic oil with improved lubricating properties). Tribologia 2009; 2. https://t.tribologia.eu/resources/html/article/details?id=165886 [accessed 09 January 2026].
16. Sliwinski P. Satellite pump and motor. Machines Technologies Materials 2014; 8(9): 8-11. https://stumejournals.com/journals/mtm/2014/9/8 [accessed 15 December 2025].
17. Sliwinski P. Influence of operating pressure on the durability of a satellite hydraulic motor supplied by rapeseed oil. Scientific Reports 2024; 14: 10441. https://doi.org/10.1038/s41598-024-61072-9.
18. Lubinski J, Sliwinski P. Multi parameter sliding test result evaluation for the selection of material pair for wear resistant components of a hydraulic motor dedicated for use with environmentally friendly working fluids. *Solid State Phenomena* 2015; 225: 115-122. https://doi.org/10.4028/www.scientific.net/SSP.225.115.
19. Osiecki L. New generation of the satellite hydraulic pumps. Journal of Mechanical and Energy Engineering 2019; 3(4): 309-314. https://doi.org/10.30464/jmee.2019.3.4.309.
20. Osiecki L. Rozwój konstrukcji pomp satelitowych (eng. Development of satellite pump structures). *Napędy i Sterowanie* 2018; 12: 84-88. http://nis.com.pl/userfiles/editor/nauka/122018_n/Osiecki.pdf [accessed 15 December 2025].
21. Wang C, Luan Z H, Gao W P. Design of pitch curve of internal-curved planet gear pump strain in type N-G-W based on three-order ellipse.

Advanced Materials Research 2013; 787: 567-571. https://doi.org/10.4028/www.scientific.net/amr.787.567.

22. Sliwinski P. The methodology of design of satellite working mechanism of positive displacement machine. *Scientific Reports* 2022; 12: 13685. https://doi.org/10.1038/s41598-022-18093-z.
23. Zhang B, Song S, Jing C, Xiang D. Displacement prediction and optimization of a non-circular planetary gear hydraulic motor. *Advances in Mechanical Engineering* 2021; 13(11): 1-13. https://doi.org/10.1177/16878140211062690.
24. Volkov G, Fadyushin D, Vedernikov M. Geometric calculation of non-circular gear segments of the planetary mechanism in rotary hydraulic machines. *E3S Web of Conferences* 2023; 389: 01017. https://doi.org/10.1051/e3sconf/202338901017.
25. Kurasov D. Geometric calculation of planetary rotor hydraulic machines. *IOP Conference Series: Materials Science and Engineering* 2020; 862: 032108. https://doi.org/10.1088/1757-899X/862/3/032108.
26. Liu Y, Fu X, Wei Y, Li D. Parametric design and motion simulation analysis of non-circular gear planetary gear train. *Journal of Mechanical Transmission* 2021; 45(8): 70-75. https://qikan.cmes.org/jxcd/EN/10.16578/j.issn.1004.2539.2021.08.010 [accessed 07 December 2025]. doi: 10.16578/j.issn.1004.2539.2021.08.010.
27. Wang K, Gao Z, Chen G, Guo M. Tooth profile construction and experimental verification of non-circular gear based on double arc active design. *Applied Sciences* 2023; 13(19): 10566. https://doi.org/10.3390/app131910566.
28. Li D, Liu Y, Gong J, Wang T. Design of a noncircular planetary gear mechanism for hydraulic motor. *Mathematical Problems in Engineering* 2021; 5510521. https://doi.org/10.1155/2021/5510521.
29. Kujawski M. *Mechanizmy obiegowe z nieokrągłymi kołami zębatymi, podstawy projektowania i wykonania* (eng. *Circulation mechanisms with non-circular gears: the basics of design and manufacturing*). Poznan University of Technology Publishing House; 1992.
30. Sliwinski P. The influence of water and mineral oil on volumetric losses in the displacement pump for offshore and marine applications. *Polish Maritime Research* 2019; 26(2): 173-182. https://doi.org/10.2478/pomr-2019-0037.
31. Sliwinski P. The influence of water and mineral oil on mechanical losses in the displacement pump for offshore and marine applications. *Polish Maritime Research* 2018; 25(s1): 178-188. https://doi.org/10.2478/pomr-2018-0040.
32. Oshima S, Hiranao T. Investigation for output torque of a low pressure water hydraulic planetary gear motor. *Ventil (Ljubljana)* 2012; 18(1): 26-35. http://www.dlib.si/?URN=URN:NBN:SI:doc-0500MONK [accessed 18 December 2025].
33. Sliwinski P. The influence of water and mineral oil on volumetric losses in a hydraulic motor. *Polish Maritime Research* 2017; 24(s1): 213-223. https://doi.org/10.1515/pomr-2017-0041.
34. Sliwinski P. The influence of water and mineral oil on mechanical losses in a hydraulic motor for offshore and marine applications. *Polish Maritime Research 2020*; 27(2): 125-135. https://doi.org/10.2478/pomr-2020-0034.
35. Panchenko A, Voloshina A, Antoshchenkov R, Halych I, Glowacki S. Experimental studies of the wear on the rotors' working surfaces of a planetary hydraulic motor. In: *Advanced Manufacturing Processes V. InterPartner 2023*. Lecture Notes in Mechanical Engineering. Springer, Cham; 2023. https://doi.org/10.1007/978-3-031-42778-7_46.
36. Voloshina A, Panchenko A, Titova O, Milaeva I, Pastushenko A. Prediction of changes in the output characteristics of the planetary hydraulic motor. In: *Advanced Manufacturing Processes II. InterPartner 2020*. Lecture Notes in Mechanical Engineering. Springer, Cham; 2020. https://doi.org/10.1007/978-3-030-68014-5_72.
37. Sliwinski P. Influence of geometrical and operational parameters on tooth wear in the working mechanism of a satellite motor. *Scientific Reports* 2023; 13: 17028. https://www.nature.com/articles/s41598-023-44319-9.
38. Szkodo M, Stanisławska A, Sliwinski P. On the durability of the hydraulic satellite motor working mechanism in overload condition. *Advances in Materials Science* 2016; 16(1): 35-46. https://doi.org/10.1515/adms-2016-0004.
39. Sliwinski P. Geometric working volume of a satellite positive displacement machine. *Scientific Reports* 2024; 14: 11195. https://doi.org/10.1038/s41598-024-61773-1.
40. Sliwinski P. The influence of pressure drop on the working volume of a hydraulic motor. *Eksploatacja i Niezawodnosc – Maintenance and Reliability* 2022; 24(4). https://doi.org/10.17531/ein.2022.4.15.
41. Sliwinski P. Determination of the theoretical and actual working volume of a hydraulic motor – Part II (The method based on the characteristics of effective absorbency of the motor). *Energies* 2021; 14(6): 1648. https://doi.org/10.3390/en14061648.
42. Sliwinski P. Determination of the theoretical and actual working volume of a hydraulic motor. *Energies* 2020; 13(22): 5933.

https://doi.org/10.3390/en13225933.

43. Sliwinski P. Influence of water and mineral oil on the leaks in satellite motor commutation unit clearances. *Polish Maritime Research* 2017; 24(3): 58-67. https://doi.org/10.1515/pomr-2017-0090.
44. Sliwinski P. & Patrosz P. Methods of determining pressure drop in internal channels of a hydraulic motor. *Energies* 2021; 14(18): 5669. https://doi.org/10.3390/en14185669.
45. Osiecki A. *Hydrostatyczny napęd maszyn*. WNT, Warszawa; 2021.
46. Banaszek A. Calculations of performance characteristics of submerged cargo pumps with hydraulic drive and constant torque controllers, taking into account the energy efficiency of the drive motor. *Energies* 2024; 17(22): 5592. https://doi.org/10.3390/en17225592.
47. Parrilla J, Cortes C. Modelling of droplet burning for rapeseed oil as liquid fuel. *Renevable Energy and Power Quality Journal* 2007; 5(1): 79-86. https://doi.org/10.24084/repqj05.221.
48. Rasep Z, Yazid M, Samion S, Paiman Z, Asral A. Rapeseed oil-based lubricant in hydrodynamic journal bearing: A computational fluid dynamics approach. *CFD Letters* 2025; 17(8): 204-216. https://doi.org/10.37934/cfdl.17.8.204216.